Stabilization and Tracking for P/PI Combustion Control over a Communication Channel ⋆

Hugo O. Garcés * **Alejandro J. Rojas** ** **Daniel Sbarbaro** **

* *Computer Science Department, Universidad Católica de la Santísima Concepción, Concepción, 4090541 Chile, (e-mail: hugogarces@ucsc.cl).*
** *Electrical Engineering Department, Universidad de Concepción, Concepción, 4070386 Chile (e-mail: arojasn@udec.cl, dsbarbar@udec.cl)*

Abstract: In the present work, motivated by the recent inclusion of optical variables in combustion processes, we consider the control of a reduced Hammerstein plant model over an additive white noise (AWN) channel located at the feedback path. For comparison, assuming uncertainty in the knowledge of the static nonlinearity of the Hammerstein plant model, we first propose in a one degree-of-freedom (DOF) scheme, the design of a proportional controller for robust stability. We then introduce a PI controller, in a 3 DOF scheme, to achieve not only robust stability, but also AWN channel Signal-to-Noise Ratio (SNR) minimization and setpoint first moment tracking.

Keywords: Communication control applications. Control system design. Discrete digital dynamic control. Feedback control. P and PI controllers. Networked Control Systems.

1. INTRODUCTION

For the last two decades the research area of Networked Control Systems (NCS) has concentrated the research interest of the control community, (J.Chen et al., 2011). Theoretical developments have proceeded apace based on information theory (Nair and Evans, 2004; Martins and Dahleh, 2008), optimization and linear control (Elia, 2004; Braslavsky et al., 2007; Rojas, 2012), multivariable and multiagent approaches (Jadbabaie et al., 2003; Middleton and Braslavsky, 2010; Knorn et al., 2016) and more recently event-triggered control (Heemels et al., 2012; da Silva Jr. et al., 2014; Campos-Delgado et al., 2015). All of the previous theoretical results and more, are now the basis for an informed control practice, revisiting established control processes, as well as facing new and demanding ones, toward achieving increased performance.

Such a revisited process is the combustion process, ubiquitous in most industrial setups Ballester and Garcia-Armingol (2010), which has recently benefited with the addition of optic based sensors Huang et al. (2010); Garces et al. (2016a). Commonly, combustion processes have their flue gasses monitored through analyzers or chromatographs, which inevitably introduce transport time-delays in the plant models and a biased measurement (Kamimoto et al., 2016; Baukal, 2010). On the other hand, optical measurements of the flame can be performed in-situ, avoiding the transport time-delay and providing a more accurate description of the combustion real time status (Ballester and Garcia-Armingol, 2010). Albeit, the obtained measurement is ideally transmitted through a communication channel, see Figure 1, avoiding unnecessary and prone to malfunction cabling due to the harsh environment and demanding conditions close to the furnace.

In Garces et al. (2016b, 2015) it is argued that for such combustion processes, monitored through optic based sensors, an Hammerstein first order model is representative of the real process, under the hypothesis of a mild nonlinearity in the stationary response of the optical measurements. Since the linear part of the plant model is a first order system, this motivate the use of P/PI controller. On the other hand, the input static nonlinearity (characteristic of an Hammerstein model) is treated in Alonge et al. (2015); Gao et al. (2015); Guo et al. (2015); Sun et al. (2009) with a 2 degree-of-freedom (DOF) controller scheme.

In our first contribution, we offer explicitly the design requirement for robust stability and its trade-off with the AWN channel SNR requirement when using a P controller.

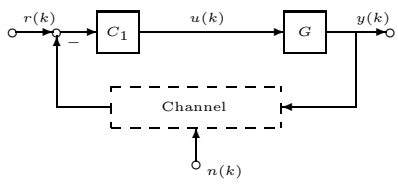

Fig. 1. Controlled combustion process scheme.

⋆ Hugo Garcés acknowledge the support of Dirección de Investigación e Innovación at Universidad Católica de la Santísima Concepción. Alejandro Rojas is grateful for the support from the Chilean Research Agency CONICYT, through Project Grant FONDECYT Regular No. 1150116 and Basal Project FB0008.

Our second contribution extends the previous to a PI controller in a 2 DOF scheme that solves the trade-off between robust stability and AWN channel SNR reduction.

In our third and last contribution we consider a 3 DOF scheme to the setpoint tracking objective, and thus highlight the trade-off between robust performance and tracking.

The significance of this work is to present a controller design strategy for optical measurements in a combustion process, to fill the gap between instrumentation systems and a feedback operation to increase energy efficiency or reduce the pollutants emissions in a complex operation, subjected to more restricted profit margins and fuels with non-constant composition.

This paper is organized as follows. Section 2 presents the standing assumptions behind this work, briefly reviewing the proposed plant model and the channel SNR definition. Section 3 derives the design requirements for a P controller to achieve robust stability. Section 4 extends the results in two directions by considering now a PI controller in a 2DOF scheme achieving robust stability and channel SNR reduction. Section 5 introduces a 3DOF scheme, together with the established PI controller, to highlight the trade-off between Robust stability, AWN channel SNR reduction and setpoint tracking. Conclusions are given in Section 6. All control results in this preliminary work are simulation based, we expect to achieve experimental confirmation at a later stage.

2. PRELIMINARIES

In this section we present the standing assumptions for this work.

2.1 Assumptions

Plant model: In Garces et al. (2016b, 2015) it has been established that a Hammerstein first order model can be a reasonable representation of an optically sensed combustion process

$$y(z) = \frac{K_G}{\alpha z - 1} f(u), \tag{1}$$

where $K_G > 0$ and $\alpha > 1$ are the plant model gain and time constant, whilst $f(u)$ is the input static nonlinearity. The signal $y(k)$ corresponds to the measured total radiation $Rad_t(k)$ and the input signal $u(k)$ to the percentage of fan speed $\lambda(k$ injecting air into the combustion chamber. In Figure 2 we show the scatter plot and average value of stationary total radiation $Rad_t(\infty)$ measured in a ladle furnace preheating process (described in Samuelsson and Sohlberg (2010); Zabadal et al. (2004)), where the nonlinear static response is verified as function of the stationary value of fan speed $\lambda(\infty)$. A schematic of optically sensed ladle furnace preheating process is presented in Figure 3 where the main stages of measurements are summarized as the field flame spectra from the flame measured with the spectrometer and the spectral processing stage where the optical variables are finally calculated.

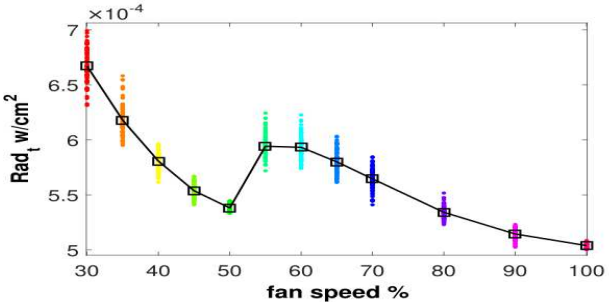

Fig. 2. Scatter plot of optically sensed ladle furnace preheating process.

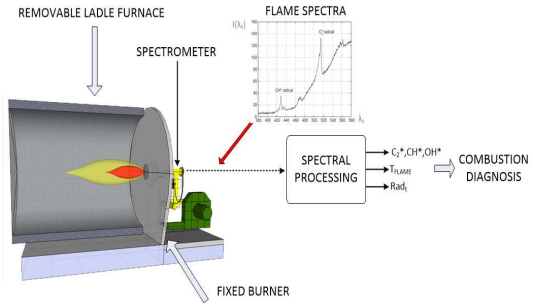

Fig. 3. Schematic of ladle furnace optically sensed.

- **Channel model**: The channel model is in general characterized by the admissible channel input power level $\mathcal{P}$ and the channel additive noise process $n(k)$.
- **Channel additive noise process**: The channel additive noise scalar process $n(k)$ is a zero-mean, i.i.d., white noise process with known variance σ^2.
- **Setpoint process**: the setpoint process is an i.i.d. Gaussian white noise process with mean μ_r and variance σ_r^2, independent of the channel additive noise process $n(k)$.

From Figure 1 we assume that the controller C_1 is such that the output feedback system is stable in the sense that for any distribution of initial conditions, the distribution of all signals in the loop will converge to a stationary distribution. The power of the channel input, defined by $\|s\|_{Pow}^2 \triangleq \lim_{k\to\infty} \mathcal{E}\left\{s^2(k)\right\}$, is then required to satisfy a user defined power constraint $\mathcal{P}$. Under the stationarity assumption presented in (Åström, 1970, §4.4), the power of the channel input can then be computed as $\|s\|_{Pow}^2 = \|T_{sr}(z)\|_2^2 \left(\sigma_r^2 + \mu_r^2\right) + \|T_{sn}(z)\|_2^2 \sigma^2$, where the H_2 norm is defined as

$$\left\|T_{\{\cdot\}}(z)\right\|_2^2 = \frac{1}{2\pi} \int_{-\pi}^{\pi} T_{\{\cdot\}}(e^{j\omega}) T_{\cdot}^H(e^{j\omega}) d\omega$$

The power constraint at the channel input can be then redefined as an SNR constraint $\frac{\mathcal{P}}{\sigma^2}$ which must be satisfied by the squared H_2 norm of $T_{sr}(z)$ and $T_{sn}(z)$

$$\frac{\mathcal{P}}{\sigma^2} > \|T_{sr}(z)\|_2^2 \frac{\sigma_r^2 + \mu_r^2}{\sigma^2} + \|T_{sn}(z)\|_2^2 . \tag{2}$$

From (2) we then have bound on the AWN channel SNR.

We treat the partial knowledge of $f(u)$, represented by $\hat{f}(\cdot)$, in a worst case scenario for which we define

$$\gamma = \max_{v} \left[f\left(\hat{f}^{-1}(v)\right)\right]. \tag{3}$$

The inner feedback loop is then analyzed for this worst-case scenario, see for example Figure 5 for the case $C_1 = K_p$, with γ in place.

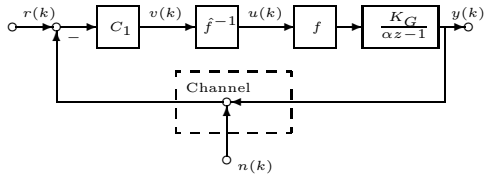

Fig. 4. 1 DOF configuration for a Hammerstein first order model over an AWN channel.

A sufficient condition for robust stability, assuming a nominal plant model G_o and a real plant model $G = G_o(1 + G_\Delta)$ can be inferred for example from (Goodwin et al., 2001, Theorem 5.3), as $\|T_o\|_\infty \|G_\Delta\|_\infty < 1$. In the previous expression $T_o = G_o C_1/(1 + G_o C_1)$ is the nominal complementary sensitivity, that is considering the nominal plant model G_o. Applied to the case under study, we recognize $G_\Delta = \gamma - 1$ and thus the condition

$$\|T_o\|_\infty |\gamma - 1| < 1 \tag{4}$$

is sufficient for robust stability. If we wish to achieve robust performance is again sufficient to increase the demand on the above condition as $\|T_o\|_\infty |\gamma - 1| << 1$.

3. 1 DOF ROBUST P CONTROL

In this section we consider the use of a proportional controller K_p in place of C_1 in Figure 4. More so, we discuss the design of K_p for the worst case scenario of mismatch knowledge on the input static nonlinearity, see Figure 5. We start by considering the nominal complementary sensitivity function resulting from a proportional controller

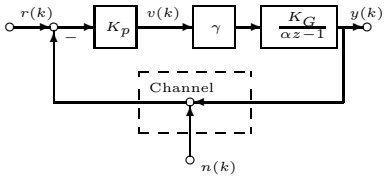

Fig. 5. 1 DOF configuration for a P robust control of Hammerstein first order model over an AWN channel.

$$T_o(z) = \frac{K_p K_G}{\alpha z - 1 + K_p K_G} \tag{5}$$

From the above we can obtain the range of values of K_p that ensures nominal stability, given α and K_G

$$\frac{1 - |\alpha|}{K_G} < K_p < \frac{1 + |\alpha|}{K_G} \tag{6}$$

Observe that, under the assumption proposed in Section 2 of $\alpha, K_G > 0$, the range of K_p spans negative and positive values. We proceed now by considering the channel SNR resulting for the nominal case. As explained in Section 2, the channel SNR is lower bounded by the expression

$$\|T_o\|_2^2 \left(\frac{\sigma_r^2 + \mu^2}{\sigma^2} + 1 \right) = \frac{K_G^2 K_p^2}{\alpha^2 - (1 - K_G K_p)^2} \left(\frac{\sigma_r^2 + \mu_r^2}{\sigma^2} + 1 \right) \tag{7}$$

As expected, as K_p approaches any of the extreme values for stability, the above lower bound tends to infinity. Also,

K_p^2	$K_G^2(2-\gamma)\gamma$	$(\alpha+1)^2$
K_p^1	$-2K_G(\alpha+1)$	0
K_p^0	$(\alpha+1)^2$	

Table 1. Routh Hurwitz algorithm on K_p.

it is clear that as $K_p \to 0$, then this SNR lower bound tends to zero, which is correct in so far the proposed linear part of the plant model is stable, $\alpha > 1$. On the other hand, if $\alpha < 1$, it is not difficult to verify that the minimum value of $\|T_o\|_2^2$ is given by $(1 - \alpha^2)/\alpha^2$ which is in agreement, for example, with (Rojas, 2012, Theorem 2). For robust stability, in light of Equation (4), we need to study the H_∞ norm of T_o. In general a closed-form expression for this type of norm is not readily available. However, in this occasion this is possible due to the rather simple expression for $T_o(z)$ we are considering in this section. Nevertheless, there are two cases to study depending on the value of the product $K_p K_G$. Specifically, for

$$K_p K_G > 1 \tag{8}$$

the H_∞ norm of $T_o(z)$ is then

$$\|T_o\|_\infty = \frac{|K_p K_G|}{\sqrt{\alpha^2 + (K_p K_G - 1)(K_p K_G - 1 - 2\alpha)}} \tag{9}$$

Since we want to impose by design the condition in Equation (4), this result in the following equation

$$0 < K_G^2(2-\gamma)\gamma \cdot K_p^2 - 2K_G(\alpha+1) \cdot K_p + (\alpha+1)^2 = K_G^2(2-\gamma)\gamma(K_p - K_{p1})(K_p - K_{p2}) \tag{10}$$

A Routh-Hurwitz argument, see Table 1, identifies both K_{p1} and K_{p2} as positive roots. Assuming $0 < K_{p1} < K_{p2}$ we expect K_{p1} to be an upper bound on K_p for robust stability.

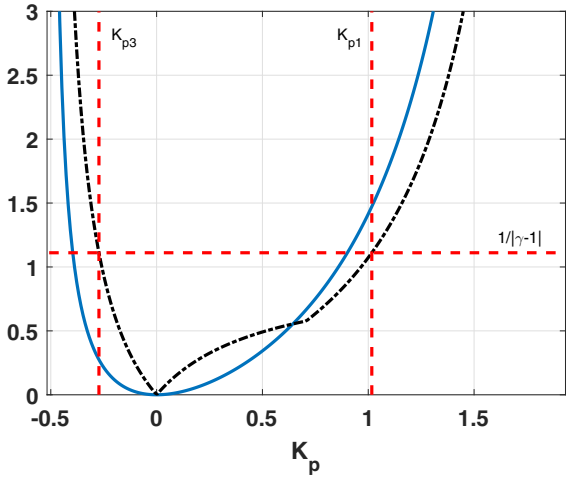

Fig. 6. AWN channel SNR, blue solid line, and H_∞ norm of the nominal complementary sensitivity $T_o(z)$, black dash-dotted line.

The second case, to complete the study on the H_∞ norm of $T_o(z)$ is imposed by

$$K_p K_G \leq 1 \tag{11}$$

which results in an expression for $\|T_o\|_\infty$ of

$$\|T_o\|_\infty = \frac{|K_p K_G|}{\sqrt{\alpha^2 + (K_p K_G - 1)(K_p K_G - 1 + 2\alpha)}} \tag{12}$$

Again, the above norm expression, together with Equation (4) lead us to the following inequality

$$0 < K_G^2(2-\gamma)\gamma \cdot K_p^2 - 2K_G(-\alpha+1)\cdot K_p + (-\alpha+1)^2 = K_G^2(2-\gamma)\gamma(K_p - K_{p3})(K_p - K_{p4}) \quad (13)$$

A similar Routh- Hurwitz, not presented, identifies K_{p3} and K_{p4} as negative roots. Assuming $K_{p4} < K_{p3} < 0$ we now expect K_{p3} to be a lower bound on K_p for robust stability. That is, in conclusion, we have for robust stability, the requirement on K_p of

$$K_{p3} < K_p < K_{p1} \quad (14)$$

To better understand the obtained expressions for the SNR reduction and robust stability we present next an example.

Example 1. In this example we consider $K_G = \sqrt{2}$, $\alpha = \sqrt{3}$, $\sigma_r^2 + \mu_r^2 = \sigma^2 = 1$ and $\gamma = 0.1$. The resulting expressions for this example are presented in Figure 6. The AWN channel SNR is shown in a blue solid line, whilst the H_∞ norm of $T_o(z)$ is shown in a black dash-dotted line. For stability the range of K_p is limited to $-0.5176 < K_p < 1.9319$, whilst for robust stability this range is further reduced to $K_{p3} = -0.2724 < K_p < 1.0168 = K_{p1}$.

The previous example highlights the limitations of using a proportional controller to solve the problems at hand, that is robust stability, SNR reduction and setpoint tracking. The proportional controller best solution for the first two is to do nothing (since the plant model is stable), and it is well known that a proportional controller is not suitable for setpoint tracking with zero steady state error.

4. 2 DOF ROBUST PI CONTROL

The last comment in the previous section motivates the proposal of using a PI controller, instead of a P controller. We also take the opportunity to analyze the introduction of a second degree of freedom in the controller solution, represented by C_2 in Figure 7. As in Freudenberg et al. (2010) we consider C_2 as a simple gain value. More so, we define $C_1(z)$ as

$$C_1(z) = \left(K_p + K_i\frac{z}{z-1}\right)\cdot\frac{1}{C_2} \quad (15)$$

that is a modified PI controller. The nominal closed-loop relationship of interest in this case is represented by

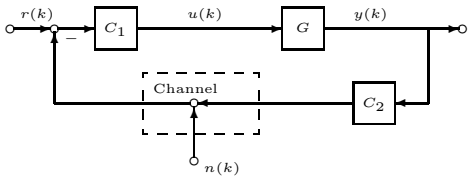

Fig. 7. General 2 DOF scheme over an AWN channel.

$$\frac{P}{\sigma^2} > \left\|\frac{C_2G_oC_1}{1+C_2G_oC_1}\right\|_2^2\left(\frac{\sigma_r^2+\mu_r^2}{\sigma^2}+1\right) \quad (16)$$

Since $C_1(z)$ contains the inverse of C_2 we have that the lower bound on the AWN channel SNR can be designed exclusively through the PI part of $C_1(z)$, that is through the user selection of K_p and K_i. From Rojas and Garces (2017), adapting the notation, we can directly quote the appropriate result for completeness, which specifies that

$$\frac{P}{\sigma^2} > \frac{2b_1b_oa_1 - (b_o^2+b_1^2)(a_o+1)}{(a_o-1)((a_o+1)^2-a_1^2)}\left(\frac{\sigma_r^2+\mu_r^2}{\sigma^2}+1\right), \quad (17)$$

with $b_1 = \frac{K_G(K_p+K_i)}{\alpha}$, $b_o = -\frac{K_GK_p}{\alpha}$, $a_1 = -1 - \frac{1}{\alpha} + \frac{K_G(K_p+K_i)}{\alpha}$, $a_o = \frac{(1-K_GK_p)}{\alpha}$.

For robust stability, on the other hand, we study the closed-loop relationship between $y(k)$ and $r(k), n(k)$ which is given by

$$y(k) = t_{ry}(k) * r(k) - t_{ry}(k) * n(k) \quad (18)$$

where the zeta transform of t_{ry} is given by

$$T_{ry}(z) = \frac{G_oC_1}{1+C_2G_oC_1} \quad (19)$$

The key observation is then that, given the proposed 2 DOF scheme and definition of $C_1(z)$, then $T_{ry}(z)$ is inversely proportional to C_2. As a consequence, as $C_2 \to \infty$, then $\|T_{ry}\|_\infty \to 0$ and thus we can satisfy the robust stability requirement imposed by γ through C_2 independently of the selection of K_p and K_i selected for SNR reduction. Finally, as we achieve steady state through a stabilizing choice of $C_1(z)$ and C_2 plus taking expectation, we obtain

$$y_{ss} = \lim_{k\to\infty} E\{y(k)\} = \lim_{k\to\infty} t_{ry} * \mu_r = \mu_r \quad (20)$$

since $E\{n(k)\} = 0$ and the presence of the integral action in $C_1(z)$. Thus, as long as $k_i \neq 0$, we can also achieve the proposed tracking objective.

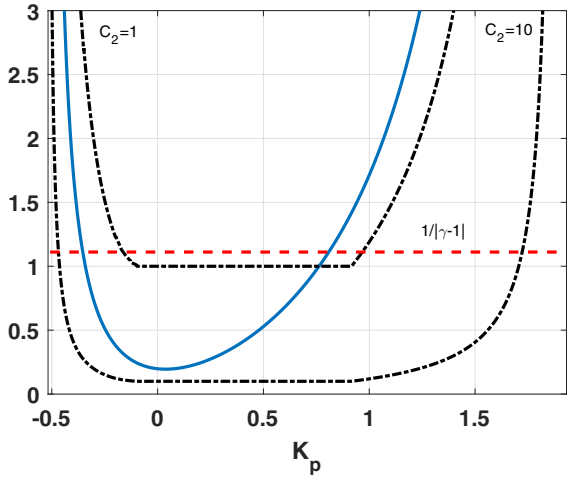

Fig. 8. AWN channel SNR, blue solid line, and H_∞ norm of the nominal complementary sensitivity $T_o(z)$, black dash-dotted line, for $C_2 = 1$ and $C_2 = 10$.

Example 2. In this example, for consistency, we also consider $K_G = \sqrt{2}$, $\alpha = \sqrt{3}$, $\sigma_r^2 = \mu_r^2 = \sigma^2 = 1$ and $\gamma = 0.1$. The integral gain K_i is selected to be 0.1. The resulting expressions for this example are presented in Figure 8. The AWN channel SNR is shown in a blue solid line, whilst the H_∞ norm of $T_o(z)$ is shown in a black dash-dotted line, for both $C_2 = 1$ and $C_2 = 10$. The range of K_p, as in the previous example and for comparison, is limited to $-0.5176 < K_p < 1.9319$. We observe that the choice of PI controller has resulted in an overall increased AWN channel SNR lower bound. We also observe, that as C_2 increases (in this case from 1 to 10) the range of values for K_p compatible with the robust stability condition (below the red dashed line) increases. This accounts for more user

freedom at the moment of deciding the AWN channel SNR. Observe also that, due to the PI structure, even for $K_p = 0$ we still have an SNR lower bound different from zero, since in this occasion, the integral part of $C_1(z)$ maintains the loop closed. Finally, Figure 9 shows the dynamic response for a sub-set of SNR values $\{0.2, 0.52, 1.68, 6.12\}$ imposed by K_p values of $\{-0.01, 0.49, 0.99, 1.49\}$, where the zero error for tracking is verified, but the dynamic response has an increased overshoot when the SNR increases. In particular, for the last value of K_p we observe a rather unacceptable overshoot of 30 % percent together with a poorly compensated oscillatory response.

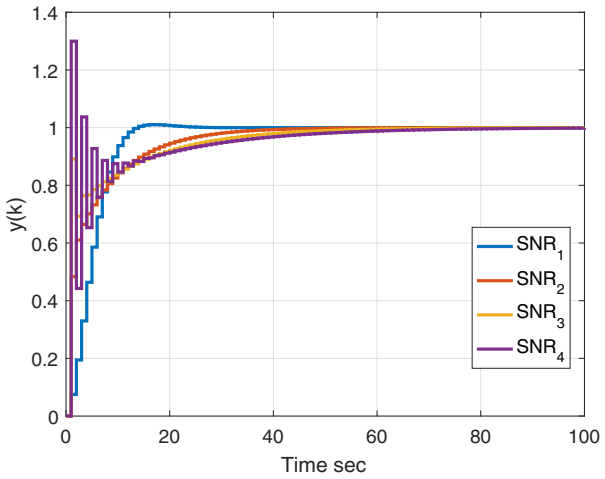

Fig. 9. Example of dynamic response for tracking and $SNR_1 = 0.1999, SNR_2 = 0.5176, SNR_3 = 1.6822, SNR_4 = 6.1168$

Another well known feature introduced by a communication channel is transmission delay. This feature can be studied directly with the present setup, see Figure 10, where we consider a one unit time delay.

The closed-loop relationship that defines the AWN channel SNR lower bound is now

$$\frac{P}{\sigma^2} > \left\| \frac{C_2 G_o C_1}{z + C_2 G_o C_1} \right\|_2^2 \left(\frac{\sigma_r^2 + \mu_r^2}{\sigma^2} + 1 \right) \tag{21}$$

For a specific PI structure for the linear part of C_1 this in turns reports

$$\frac{P}{\sigma^2} > \frac{-(b_1 - b_2)^2 \beta_1 + 2 b_1 b_2 (\alpha_1 - \beta_1)}{\alpha_2 \beta_1 - \alpha_1 \beta_2} \left(\frac{\sigma_r^2 + \mu_r^2}{\sigma^2} + 1 \right), \tag{22}$$

with $b_2 = \frac{K_G(K_p+K_i)}{\alpha}$, $b_1 = -\frac{K_G K_p}{\alpha}$, $a_2 = -\frac{\alpha_1+1}{\alpha}$, $a_1 = \frac{1+K_G(K_p+K_i)}{\alpha}$, $a_o = -\frac{K_G K_p}{\alpha}$, $\alpha_1 = a_o a_1 - a_2$, $\alpha_2 = -2a_o a_1 a_2 + a_o^2 + a_1^2 + a_2^2 - 1$, $\beta_1 = a_o^2 + a_o a_2 - a_1 - 1$ and $\beta_2 = 2(a_1 - a_o a_2)(a_o + a_2)$. We omit the proof, but as intuition would have it, for the same values of K_p, K_i, K_G and α an extra time delay increases the AWN channel SNR lower bound. Of course a transmission delay is not limited to only one unit time delay, but again, the more the transmission delay the bigger will be the AWN channel SNR lower bound and thus the overall requirement for a successful transmission over the AWN channel. The robust part of the design, when including a one time delay in the channel, follow the same approach as without it.

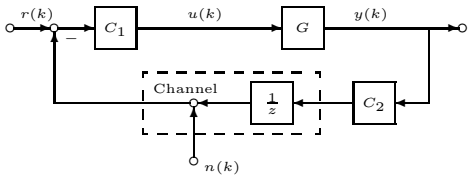

Fig. 10. General 2 DOF scheme over an AWN channel with a one unit time delay.

5. 3 DOF FOR ROBUST PERFORMANCE

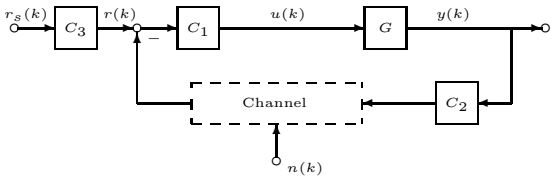

Fig. 11. General 3 DOF scheme.

In this section we consider the use of a 3 DOF scheme, see Figure 11. This approach is in line with what already proposed in Alonge et al. (2015); Gao et al. (2015); Guo et al. (2015); Sun et al. (2009), albeit for a 2 DOF scheme. The main objective is to use $C_3(z)$ to impose a desired closed-loop relationship between $y(k)$ and the pre-filtered setpoint $r_s(k)$. It is straightforward then, given $T_{obj}(z)$ as such a desired closed-loop objective, that a suitable choice for $C_3(z)$ is

$$C_3(z) = \frac{1}{C_2} \cdot T_{obj}(z) T_{ry}^{-1}(z) \tag{23}$$

For the above choice, and the scheme in Figure 11, the AWN channel SNR is now lower bounded by

$$\frac{P}{\sigma^2} > \|T_{obj}\|_2^2 \frac{\sigma_{rs}^2 + \mu_{rs}^2}{\sigma^2} + \|T_{sn}\|_2^2 \tag{24}$$

where σ_{rs} and μ_{rs} are the variance and mean, respectively, of $r_s(k)$. The AWN channel SNR lower bound is then the result of the design of $T_{sn}(s)(z)$ and the choice of $T_{obj}(z)$. For robust stability, on the other hand, we have

$$y(k) = \frac{1}{C_2} \cdot t_{obj}(k) * r(k) - t_{ry}(k) * n(k) \tag{25}$$

The key observation now is that, as long as $C_3(z)$ is inversely proportional to C_2, we can still satisfy the robust stability requirement imposed by γ through C_2, independently of the selection of K_p and K_i, assuming a PI choice for $C_1(z)$. As in the previous section, taking expectation we obtain the tracking of r_s by $y(k)$

$$y(k) = E\{\frac{1}{C_2} \cdot t_{obj}(k) * r(k) - t_{ry}(k) * n(k)\} = \frac{\mu_{rs}}{C_2} \cdot t_{obj}(k) \tag{26}$$

Therefore, with the user choice of $t_{obj}(k)$ for all k, subject to $\lim_{k\to\infty} t_{obj}(k) = C_2$, we can impose as desired, a user defined closed-loop relationship between $y(k)$ and the pre-filtered setpoint $r_s(k)$.

6. CONCLUSIONS

In the present work, motivated by the recent inclusion of optical variables in combustion processes, we have proposed different schemes for the control of a reduced Hammerstein plant model over an additive white noise

(AWN) channel located at the feedback path using P and PI controllers. We first proposed a 1 DOF scheme with a P controller to illustrate the design challenges involved. We then introduced a PI controller, in a 2 DOF and 3 DOF scheme, to achieve not only robust stability, but also AWN channel SNR reduction and setpoint first moment tracking. Future directions should consider other type of communication channel models, beyond the AWN channel, and also the inclusion of dynamical uncertainty in the linear part of the plant model.

REFERENCES

Alonge, F., Rabbeni, R., Pucci, M., and Vitale, G. (2015). Identification and Robust Control of a Quadratic DC/DC Boost Converter by Hammerstein Model. *IEEE Transactions on Industry Applications*, 51(5), 3975–3985.

Åström, K. (1970). *Introduction to Stochastic Control Theory*. Academic Press.

Ballester, J. and Garcia-Armingol, T. (2010). Diagnostic techniques for the monitoring and control of practical flames. *Progress in Energy and Combustion Science*, 36(4), 375–411.

Baukal, C.E. (2010). *Industrial combustion testing*. CRC Press.

Braslavsky, J., Middleton, R., and Freudenberg, J. (2007). Feedback Stabilisation over Signal-to-Noise Ratio Constrained Channels. *IEEE Transactions on Automatic Control*, 52(8), 1391–1403.

Campos-Delgado, D.U., Rojas, A.J., Luna-Rivera, J.M., and Gutiérrez, C.A. (2015). Event-triggered feedback for power allocation in wireless networks. *IET Control Theory & Applications*, 9(14), 2066–2074.

da Silva Jr., J., Lages, W., and D.Sbarbaro (2014). Event-triggered pi control design. In *Proceedings of the 19th IFAC World Congress*, 6947–6952. Cape Town, South Africa.

Elia, N. (2004). When Bode meets Shannon: Control oriented feedback communication schemes. *IEEE transactions on Automatic Control*, 49(9), 1477–1488.

Freudenberg, J., Middleton, R., and Solo, V. (2010). Stabilization and disturbance attenuation over a Gaussian communication channel. *IEEE Transactions on Automatic Control*, 55(3), 795–799.

Gao, X., Ren, X., Zhu, C., and Zhang, C. (2015). Identification and control for Hammerstein systems with hysteresis non-linearity. *IET Control Theory & Applications*, 9(13), 1935–1947.

Garces, H.O., Arias, L., Rojas, A.J., Carrasco, C., Fuentes, A., and Farias, O. (2016a). Radiation measurement based on spectral emissions in industrial ïňĆames. *Measurement*, 87, 62–73.

Garces, H., Rojas, A., Arias, L., and Carrasco, C. (2015). On the use of flame analysis and optical variables for an optimized operation in ladle furnace preheating process. In *2015 IEEE Multi-Conference on Systems and Control*, 269–274. Sydney, Australia. doi:10.1109/CCA.2015.7320640.

Garces, H.O., Rojas, A.J., and Arias, L.E. (2016b). Selection of nonlinear structures for total radiation modeling. In *IEEE International Conference on Automatica*, 1–5. Curico, Chile.

Goodwin, G., Graebe, S., and Salgado, M. (2001). *Control System Design*. Prentice Hall.

Guo, Y., Mao, J., and Zhou, K. (2015). Rate-Dependent Modeling and h_∞ Robust Control of GMA Based on Hammerstein Model With Preisach Operator. *IEEE Transactions on Control Systems Technology*, 23(6), 2432–2439.

Heemels, W., Johansson, K., and Tabuada, P. (2012). An introduction to event-triggered and self-triggered control. In *Proceedings of the 51th Conference on Decision and Control*, 3270 – 3285.

Huang, B., Luo, Z., and Zhou, H. (2010). Optimization of combustion based on introducing radiant energy signal in pulverized coal-fired boiler. *Fuel Processing Technology*, 91(6), 660–668.

Jadbabaie, A., Lin, J., and Morse, A. (2003). Coordination of groups of mobile autonomous agents using nearest neighbor rules. *IEEE Transactions on Automatic Control*, 48(6), 988–1001.

J.Chen, de Silva, C., S.Olariu, I.C.Paschalidis, and I.Stojmenovic (eds.) (2011). *IEEE Transactions on Automatic Control. Special issue on wireless sensor and actuator networks*, volume 56.

Kamimoto, T., Deguchi, Y., Shisawa, Y., Kitauchi, Y., and Eto, Y. (2016). Development of fuel composition measurement technology using laser diagnostics. *Applied Thermal Engineering*, 102(Supplement C), 596 – 603. doi:https://doi.org/10.1016/j.applthermaleng.2016.03.075.

Knorn, S., Chen, Z., and Middleton, R. (2016). Overview: Collective control of multiagent systems. *IEEE Transactions on Control of Network Systems*, 3(4), 334–347.

Martins, N. and Dahleh, M. (2008). Feedback Control in the Presence of Noisy Channels: "Bode-Like" Fundamental Limitations of Performance. *IEEE Transactions on Automatic Control*, 53(7), 1604–1615.

Middleton, R. and Braslavsky, J. (2010). String Instability in Classes of Linear Time Invariant Formation Control with Limited Communication Range. *IEEE Transactions on Automatic Control*, 57(7), 1519–1530.

Nair, G. and Evans, R. (2004). Stabilizability of stochastic linear systems with finite feedback data rates. *SIAM J. Control and Optimization*, 43(2), 413–436.

Rojas, A. (2012). Signal-to-noise ratio fundamental limitations in the discrete-time domain. *Systems & Control Letters*, 61(1), 55–61.

Rojas, A. and Garces, H. (2017). Signal-to-noise ratio requirements for discrete-time pid controllers. In *20th IFAC World Congress*, 2622–2627. Toulouse, France.

Samuelsson, P. and Sohlberg, B. (2010). Ode-based modelling and calibration of temperatures in steelmaking ladles. *IEEE Transactions on Control Systems Technology*, 18(2), 474–479. doi:10.1109/TCST.2009.2016668.

Sun, J., Liu, G., Chen, J., and Rees, D. (2009). Networked Predictive Control for Hammerstein-Wiener Systems via Output Feedback. In *Proceedings of the European Control Conference*, 395–399. Budapest, Hungary.

Zabadal, J., Vilhena, M., and Leite, S. (2004). Heat transfer process simulation by finite differences for online control of ladle furnaces. *Ironmaking and Steelmaking*, 31(3), 227–234. doi:10.1179/030192304225012150.